Enhancement of the Spin Hall Effect in Heavy Metal Bilayers

Haron Abdel-Raziq
Sayeef Salahuddin, Ed.
Jeffrey Bokor, Ed.

Electrical Engineering and Computer Sciences
University of California at Berkeley

Technical Report No. UCB/EECS-2016-29
http://www.eecs.berkeley.edu/Pubs/TechRpts/2016/EECS-2016-29.html

May 1, 2016

Acknowledgement

In report

Enhancement of the Spin Hall Effect in Heavy Metal Bilayers

Haron Abdel-Raziq

Research Project

Submitted to the Department of Electrical Engineering and Computer Sciences, University of California at Berkeley, in partial satisfaction of the requirements for the degree of **Master of Science, Plan II**.

Approval for the Report and Comprehensive Examination:

Committee:

Sayeef Salahuddin
Research Advisor

(Date)

* * * * * * *

Jeffrey Bokor
Second Reader

(Date)

Abstract

A series of measurements were performed in order to analyze the impact of including an additional metal (known to have a Spin Hall effect) directly below another metal with the opposite sign of the effect. Experimental data shows, at first glance, that there is an anomalous enhancement of the spin Hall angle when this extra metal layer is included. The effect was noted by observing the switching current density for several samples. Each sample with a thicker underlayer of this metal, exhibited less current density for switching, thus opening the opportunity for enhancement of the spin Hall effect through the placement of an extra underlayer of metal featuring a spin Hall effect.

Acknowledgements

First and foremost, I would like to begin by deeply thanking my professor and advisor Sayeef Salahuddin. Professor Salahuddin, you provided excellent guidance as a professor and I always found you approachable and greatly helpful with my research. I thank you for all the guidance you provided and all the support you gave to me as a student in your group.

Next, I want to give my thanks to the other students in my group. Each and every student in the Sayeef group was a fountain of knowledge and I found my lab-mates extraordinarily helpful and friendly with solving issues that might come up. Particularly, I want to give thanks to those in the experimental portion of our group. Many times I found myself stuck with a particular issue with my setup and I sought guidance from you all that helped me solve those issue.

As a student performing experiments and materials growth, I had the privilege of cooperating with the students in Professor Ramesh's group in the materials science department. I want to particular thank Yeonbae Lee, and James Clarkson for all the help provided with sputtering, wire bonding among other things. Thank you so much.

Last but not least, I would like to thank Professor Bokor for taking the time away from his busy schedule to read my master's report.

Table of Contents

1. Introduction **2**
- 1.1 Magnetic Tunnel Junctions…… 2
- 1.2 Spin-Torque Switching a Perpendicularly Polarized Magnet…… 4
- 1.3 Spin-Torque Switching with Bilayers of Spin Hall Effect Metals……. 5

2. Background **6**
- 2.1 Ferromagnets and Ferromagnetism…… 7
- 2.2 The Spin Hall Effect……... 8
- 2.3 Spin Orbit Torque Driven Switching…….. 10

3. Process Flow **13**
- 3.1 Fabrication Process Flow……..... 13
- 3.2 Measurements……. 14

4. Experiments & Results **16**
- 4.1 Main Experiments and Results……..... 16
- 4.2 Examination of Potential Problems……..... 21

5. Conclusion **24**

References **25**

1
Introduction

Advances in memory are quickly approaching a wall due to the ever-decreasing size of modern devices coupled with the difficulty in fabricating such devices. As such, new avenues for inventing similar memory, logic, and other systems are being researched. Furthermore, in the spirit of physics and research, interesting mechanisms can be discovered through the understanding of new materials systems. One such a group is ferromagnets layered with other materials. Such materials have yielded a multitude of technology including magnetic random access memory (MRAM), the fundamental magnetic tunnel junctions (MTJs), racetrack memory, and spin-based logic among others. In developing these new materials systems, one desires low power, fast switching, and stable storage.

In pursuit of meeting (and hopefully exceeding) these criteria, the spin torque mechanism of switching a ferromagnet has been researched quite heavily. This method allows magnetic based technology to move away from switching with an Oersted field generated by current flow through a small wire. The continued shrinking of devices makes this development crucial in furthering magnetic technology, since with smaller devices one also requires larger Oersted fields (and thus larger currents) to switch a magnetic element. The Oersted field is not scalable. Spin torque is more scalable as it is not as heavily dependent on size and consequently a device utilizing spin torque would need significantly less power than one that uses Oersted fields.

1.1 Magnetic Tunnel Junctions

One of the most prevalent technologies included in magnetic memory systems is the magnetic tunnel junction. This is typically a thin film stack grown to include the following: Ferromagnetic Metal/ Tunnel Barrier (Oxide) / Ferromagnetic Metal. The fundamental magnetic tunnel junction can be seen in figure 1. Note this does not contain other layers explained later. Various other materials can be included but the stack structure listed above typically makes up the basis of a magnetic tunnel junction. These original magnetic tunnel junctions utilize one ferromagnet as a fixed layer (typically referred to as the reference layer) and the other layer as a free layer (the layer which data is encoded into). Bits are encoded by way of the tunnel magnetoresistance (TMR) of the MTJ. The tunnel magnetoresistance is commonly defined as:

$$\frac{\Delta R}{R} = \frac{R_{AP} - R_P}{R_P}$$

Where R_{AP} and R_P are the anti-parallel and parallel resistances, respectively. When the magnetizations are antiparallel, the resistance is typically high. Consequently, when the magnetizations are parallel, the resistance is low. Thus, bit values of 0 and 1 can be encoded through high and low TMR values. For clearer separation between bit values of 1 and 0, a larger TMR ratio is desired. Recently, a perpendicular anisotropy magnet based MTJ has exhibited a TMR percentage of 120% [1].

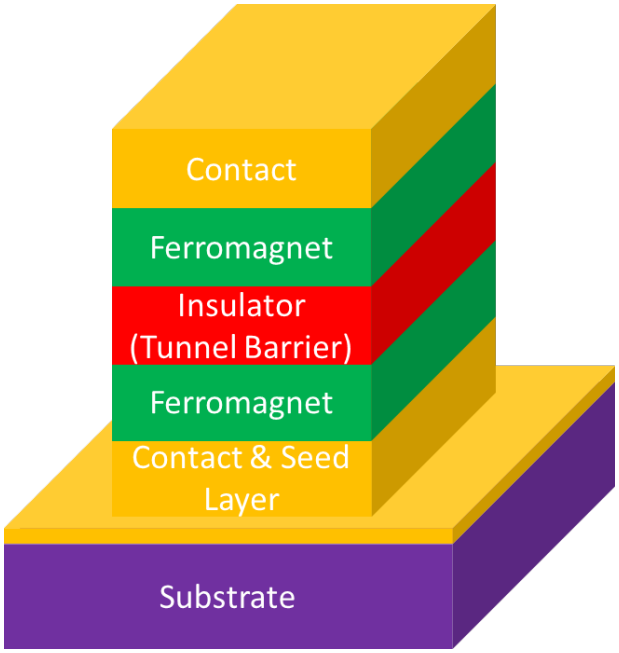

Figure 1: The typical structure of a magnetic tunnel junction stack. The layers are usually of approximately equivalent thickness, grown on top of a much thicker substrate.

MTJs have been experimented with both with the in-plane magnetic easy axes and out-of-plane magnetic easy axes (discovered more recently) [1]. One of the more salient issues with in-plane easy axis MTJs is they generally require much larger switching current due to the demagnetization energy required[1]. Consequently, perpendicular anisotropy allows for a reduction of switching current while providing thermal stability. This report will explore perpendicular anisotropy magnets and thus, their importance in MTJs is outlined here.

As mentioned, certain materials have been included in the stack in order to optimize the MTJ to reach the aforementioned TMR ratios. Such innovations include the inclusion of spin valves in the structure to stabilize the magnetization, particularly that of the reference layer[2]. This is particularly helpful for antiparallel detection, where an antiferromagnet is used to pin the magnetization of the reference layer.

The outlined benefits of perpendicular anisotropy materials motivated the spintronics community to research perpendicular anisotropy stacks taking advantage of the spin torque technique. Several materials systems have been found exhibiting this property and will be discussed in this report. Furthermore, the goal of the project undertaken and outlined here was to optimize these stacks in order to enhance the spin torque effects seen and to gain some insight on how future materials systems utilizing perpendicular magnets could be enhanced.

A clear distinction should be made here concerning the terms commonly used in research in this area, particularly spin transfer torque (STT) and spin Hall Effect spin torque (SHE-ST) as we will refer to spin orbit torque here since its origin is still in debate[3,4]. Our work more closely follows that developed by Liu et al. in [6], and thus the reason for using that origin of the spin orbit torque. Spin transfer torque was the common type of switching mechanism utilized in

magnetic tunnel junctions where an applied current would proceed through a polarizing ferromagnet layer. Once polarized, this spin current could then apply a torque to a magnet. The basic mechanism is featured figure 2. This type of torque is a result of an interaction between mobile electrons in the magnet that are spin polarized and the magnetization. The interaction can be quite strong and occurs locally[5]. That is, it only occurs in regions where the spin currents themselves flow and thus are very conducive to precise control. Spin transfer torques have been found to be both present and important in all known magnetic materials, including transition metal ferromagnets, magnetic semiconductors and oxide ferromagnets[5]. Spin orbit torque (or spin Hall Effect spin torque), on the other hand, does not involve passing a current through a polarized ferromagnetic layer at all. Rather, it utilizes the special effect of metals described later in this report to "sort" the spins in an applied current. Once the current is applied to these particular metals, a torque can be applied to a magnet from the developed spin current. This is the type of spin torque explored in this report and is the one of the main focuses of current magnetic materials research.

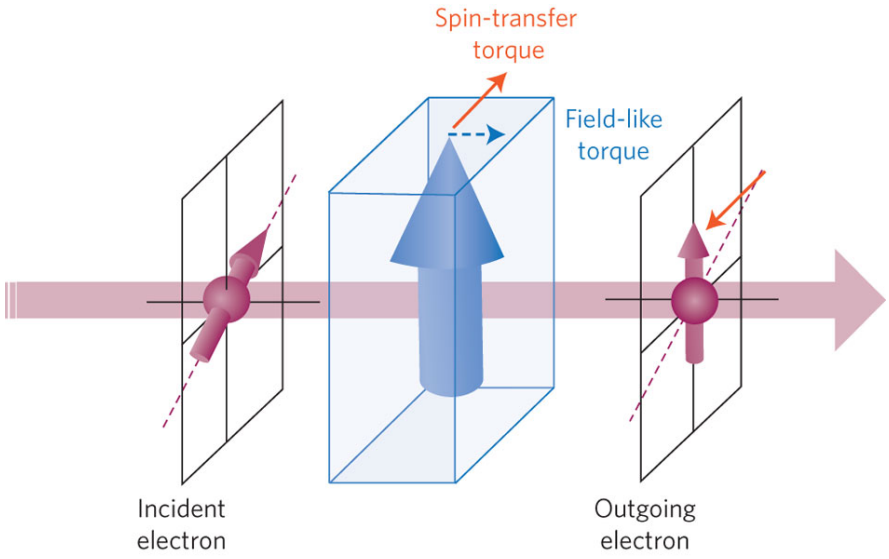

Figure 2: A spin-polarized current enters a ferromagnet. The interaction between the spin-polarized current and the magnetization causes a change in the spin direction of the outgoing electron compared with the incident electron. The difference in spin polarization causes torques on the ferromagnet, both a torque in the plane of the incident and outgoing electron spin directions (a spin-transfer torque) and a torque perpendicular to that plane, called the field-like torque. The bold vertical arrow is the magnetization of the ferromagnetic layer. Reproduced from [5].

1.2 Spin-Torque Switching a Perpendicular Anisotropy Magnet

One of the first experimental proofs of a perpendicular anisotropy magnetic tunnel junction was featured in the article by Ikeda et al. [1]. Furthering the discovery of a method for producing perpendicular anisotropy MTJs which can be switched utilizing relatively low currents requires a proper material to deliver sufficient torque. In the paper published in the journal Science by Liu et al., proof of the giant spin Hall Effect of tantalum was reported[6].

Finding a giant spin Hall Effect in tantalum was significant because this meant that tantalum, by itself a nonmagnetic materials, could apply spin torque to magnets. This is contrary to the method typically used in MTJs which involves passing a charge current through a polarizing ferromagnet layer and then through the tunnel barrier. In this original switching method, it is quite difficult to pass enough spin current through a barrier without causing some type of damage to the barrier, thus resulting in an unusable MTJ.

β-tantalum, the phase of tantalum reported as exhibiting this giant spin Hall Effect, is that which is grown by dc magnetron sputtering. This phase of tantalum is identified by its high resistivity, around a measured value of 190 μohm•cm. Figure 3 (from Liu et al.) shows the perpendicular anisotropy of the magnet and the switching of this magnet with a current through the β-tantalum.

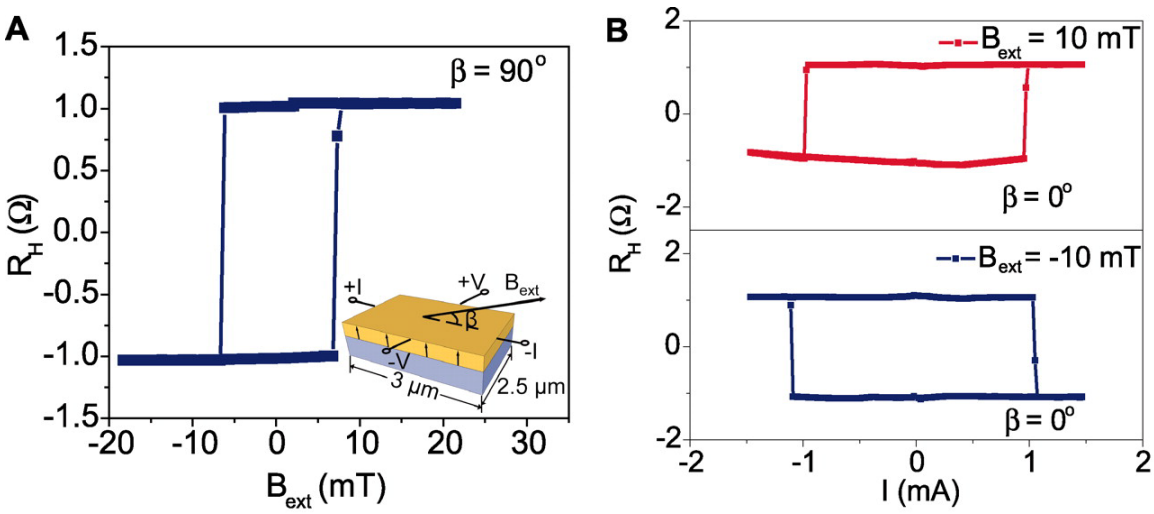

Figure 3[6]: A) The anomalous Hall Resistance (R_H) with the field applied in the easy axis (perpendicular) direction. B) The switching characteristics when a small field B_{ext} is applied parallel (or antiparallel in the bottom plot) to the current direction from Liu et al [6]

The actual stack used for the measurements made in figure 2 was substrate/Ta(4)/$Co_{40}Fe_{40}B_{20}$(1)/MgO(1.6)/Ta(1) with thicknesses in nanometers. These were then patterned into Hall bars 2.5 to 20μm wide and 3 to 200μm long. Since the discovery of the data shown in figure 3, significant research has been done on characterizing this materials system as well as others (including Pt/Co and W/CoFeB). Furthermore, research has also been done on placing a spin Hall Effect metal on either side of the magnet in order to enhance the switching (that is, to reduce the switching current required)[7]. The hope of enhancing the switching characteristics through yet another mechanism was the goal of the project reported here and the general idea is discussed next.

1.3 Spin Torque Switching with Bilayers of Spin Hall Effect Metals

Electronics used for memory, logic, and virtually every application consume a certain amount of power even in the off state. Thus, one goal of device designers is always to reduce the current used by the device. Switching current, the primary method of changing the magnetization of the free layer in an MTJ (to be used in a memory cell for example) is the quantity we seek to

reduce in spin torque based devices. The work done in [7] is one such work and was actually submitted for publication while this project was in progress. The work reported here also seeks to reduce the switching current but through a different mechanism.

This work examines the stack of Ta(2)/Pt(x)/Ta(10-x)/CoFeB(1)/MgO(2)/Ta(2) grown on a Si/SiO_2 substrate, with thicknesses in nanometers. The placement of another spin Hall Effect metal placed adjacent to the tantalum reduces the current density required to switch the magnet. The exact (physical) explanation for the anomalous enhancement observed (potentially) in the data is still not understood. However, the data shown in the results section of the report suggests that there may be in fact an enhancement when utilizing bi-layers of spin Hall Effect metals (with opposite sign of the spin Hall Effect). Potential pitfalls of this data will be discussed and the results along with more details will be discussed later in this report.

2
Background

2.1 Ferromagnets and Ferromagnetism

Ferromagnetic materials, in contrast to paramagnetic and diamagnetic materials, can sustain large and permanent magnetizations due to the exchange interaction. This makes them useful materials as they can maintain a magnetization without an applied field present. Although it may take a field to align the dipoles in the material, once aligned, the dipoles tend to remain this way barring other perturbations.

A typical ferromagnet can be schematically drawn as featured in figure 4 (with the features not to scale). Prior to experiencing a magnetic field aligning the moments, the ferromagnet will have several domains (each separated by domain walls, a topic researched heavily but not discussed in this report) with the moments in each domain aligned in a certain direction. Within the domain wall, the dipoles typically rotate from one end of the wall to the other (see figure 4). The moments in the different domains need not be aligned prior to the application of a magnetic field. However, once a magnetic field is applied, the domains with dipoles in the same direction as the field will tend to grow while other domains will tend to shrink until there is one domain with moments aligned with the field. The shrinking of these moments can be seen in figure 5a.

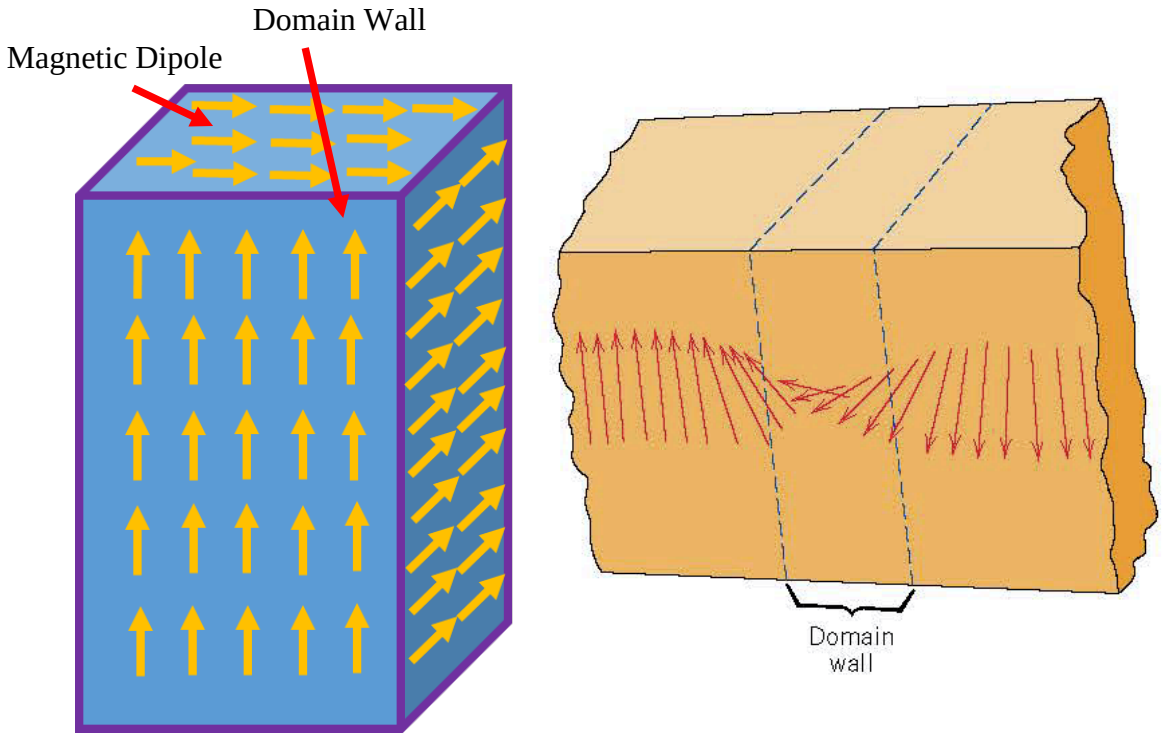

Figure 4: (Left) Schematic representation of a ferromagnet. The yellow arrows indicate magnetic dipoles and the purple lines represent the domain walls. (Right)[8] Representation of magnetic dipoles in a ferromagnet and their rotation across the domain wall [Callister Materials Science and Engineering: An Introduction].

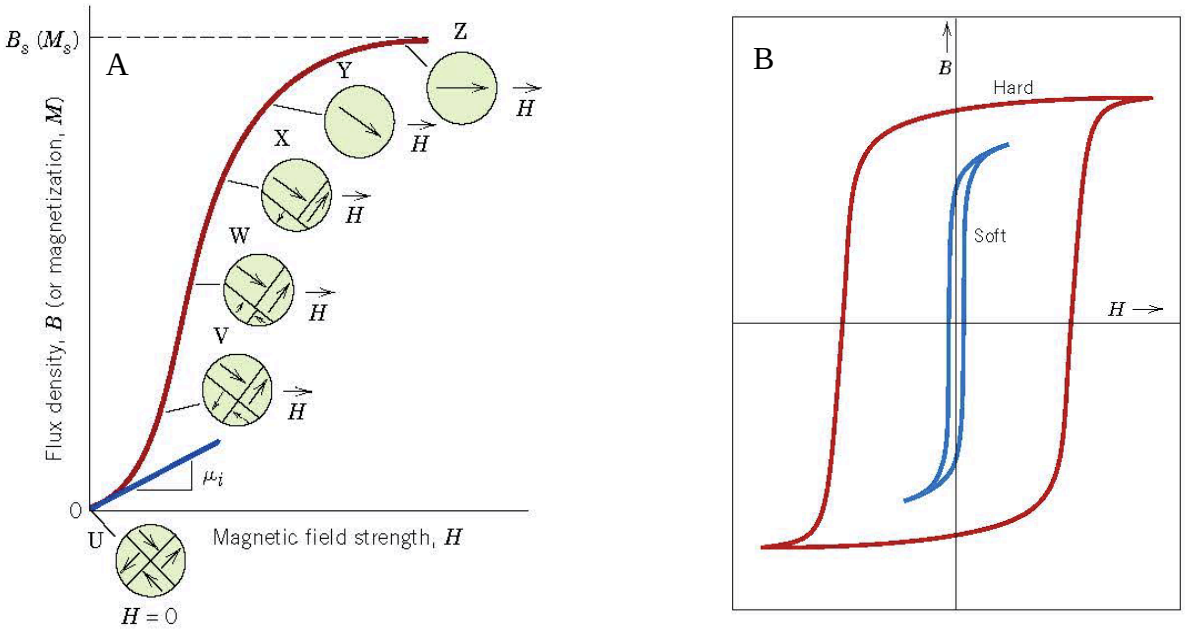

Figure 5[8]. A) Magnetization curve showing flux density B (or magnetization, different by only a constant) vs. the applied field. The curve shows how domains in the direction of the field grow with an increasing applied field. B) Curve showing the hysteresis curve for hard and soft magnetic materials [Callister Materials Science and Engineering: An Introduction].

Once a field of any magnitude is applied, the sample begins exhibiting a magnetization M along the direction of the field. With increasing field, this value M will continue to grow until the saturation magnetization, M_s, is reached. Once saturated, the magnetization will not increase further. Ferromagnets typically exhibit a large enough magnetization such that the induction:

$$B = \mu H + \mu M$$

where H is the applied field, μ is the permeability of the material, and M is the magnetization.

The ability of ferromagnets to hold large, permanent magnetizations in one of two directions is one of the key properties making them useful for memory. In conjunction with the properties of switching explained in this report, these “up” and “down” magnetizations allow one to store bits 0 and 1, thus making ferromagnets a clear choice in developing new memory technology.

2.2 The Spin Hall Effect

Qualitatively, the spin Hall Effect describes the deflection of electrons with opposite spin, in opposite directions, transverse to an input unpolarized charge current. The spin Hall Effect explored in this report is typically exhibited by heavy metals such as platinum, tantalum, or tungsten. The origin of the spin Hall Effect is due to the spin orbit coupling experienced by the conduction electrons. Conduction electrons traversing these metals will experience the spin Hall Effect and deflect based on the direction of their spins. The spin Hall Effect, as explored here,

ultimately causes a spin current to be absorbed by an adjacent ferromagnet thus applying a torque on the magnetic moment of the magnet. Through this mechanism, switching of the ferromagnet's magnetic moment can occur[6].

A detailed derivation involving the spin orbit coupling interaction and the velocity of conduction electrons can be found in [9]. The derivation yields the following result for the spin current:

$$\overrightarrow{J_s} = \frac{\hbar}{2e}\theta_{SHE}(\hat{y} \times \overrightarrow{J_e})$$

where $\overrightarrow{J_s}$ is the spin current density, θ_{SHE} is the spin Hall angle, $\hat{y}$ is the direction of spin polarization of the electrons at the top surface of the heavy metal layer, and $\overrightarrow{J_e}$ is the charge current density. The spin Hall angle of 4d and 5d transition metals such as Niobium (Nb), Tantalum (Ta), Molybdenum (Mo), Palladium (Pd), and platinum (Pt) has been experimentally found to change sign based on the number of d shell electrons[11].

Referencing [9], if the heavy metal exhibiting a SHE is placed on the substrate with no adjacent layers and a current is passed through causing the generation of a spin current, the boundary conditions state that the spin current must be zero at the top and bottom surfaces of the heavy metal. This implies that the component of spin current caused by the spin Hall Effect must be cancelled by a different spin current. Similar to the equilibrium situation in a MOS-transistor where the drift current is cancelled by the diffusion current, a spin diffusion current flows opposite the spin Hall effect spin current due to the net spin accumulation across the heavy metal layer. The net spin accumulation across a particular material is given by $\mu^{\uparrow}(z) - \mu^{\downarrow}(z)$ where $\mu^{\uparrow}(z)$ is the chemical potential for electrons with spin in the +x direction and $\mu^{\downarrow}(z)$ is the chemical potential for electrons with spin in the –x direction[11]. Figure 6 shows how the spin Hall Effect distributes the spins in a spin Hall metal, provided a charge current has been applied.

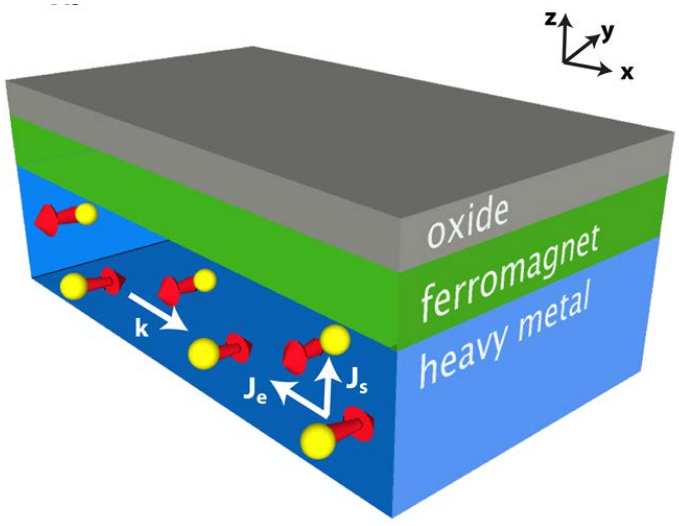

Figure 6[9]: A schematic representation of the spin Hall Effect with electrons having a velocity Proportional to $\vec{k}$ (+x direction in this image). The effect causes the electrons to deflect either in the +z or –z depending on their spin polarization. This causes a spin current transverse to the charge current flowing.

Accounting for the chemical potentials due to the gradient of spins in the material, we have a spin current equation (again similar to the total current equation of a MOS-transistor):

$$\overrightarrow{J_s} = \frac{\hbar}{2e}\theta_{SHE}\left(\hat{y} \times \overrightarrow{J_e}\right) + \overrightarrow{\nabla}(\mu^{\uparrow}(z) - \mu^{\downarrow}(z))$$

Where $\overrightarrow{\nabla}(\mu^{\uparrow}(z) - \mu^{\downarrow}(z))$ is the gradient of the difference of the potentials, as we would expect for a diffusion current term.

The situation is somewhat different if a ferromagnetic metal is situated adjacent to the heavy metal. Again referencing [6], the boundary condition no longer requires that the spin current be zero at that interface. Now, the spin current is absorbed by the ferromagnet. The spin-polarized electrons diffuse into the ferromagnet and align with the magnetization of the ferromagnet due to the strong exchange coupling. This results in a spin torque on the ferromagnet equal to the spatial change of the spin current inside the ferromagnet compensated by the spin relaxation term: $\frac{1}{V}\int dV(-\vec{\nabla}.\vec{J_s} - \frac{1}{\tau_{SF}}\vec{M})$, where V is the volume of the ferromagnetic layer, $\vec{J_s}$ is the spin current, $\vec{M}$ is the magnetization of the ferromagnet and τ_{SF} is the spin relaxation time[13].

2.3 Spin Orbit Torque Driven Switching

The first reported observation of spin orbit torque was by Miron et al. on the spin orbit torque switching of a ferromagnet in a heavy metal/ferromagnet/oxide trilayer[13, 14]. Miron et al. attributed the switching featured in their devices to switching due to the Rashba Effect, not discussed here. For more details and a more thorough discussion, see references 9, 13, and 14. As mentioned, this report largely considers the spin orbit torque (spin Hall Effect spin torque) theory of switching the magnet due to its presence in published articles utilizing similar materials systems as that explored here.

Liu et al.[15] obtained deterministic switching on a perpendicularly polarized magnet. Their devices were 20μm by 200μm Hall bars made from the stack of Pt(2)/Co(0.6)/AlO_x stack, with thicknesses in nanometers. Similar devices were tested by Miron et al. This experiment was different in that the switching was explained to have occurred as a result of the spin Hall Effect spin torque, with a full explanation included in the article. In the presence of an external magnetic field, a current pulse in the direction of the field generates hysteretic magnetic switching between "up" and "down" states (figure 7a and b). Changing the direction of the field results in a change of the switching direction as seen in the figure. The sample is shown in figure 7c and the hysteresis curve showing it is indeed an out of plane sample is included in figure 7d. The spin current dynamics can be explained in terms of the coordinate system and schematic in figure 7e. A current pulse applied in in the +y direction results in a spin accumulation of electrons in the +x direction at the interface of platinum and the cobalt magnet. Following the explanation in [9], assuming the cobalt layer is uniformly magnetized (this is the single domain assumption also known as the Stoner Wolfarth model[15]) and has a magnetization $\vec{M}$, the spin torque acting on the ferromagnetic cobalt layer is given by $\frac{\hbar}{2eM_s t}J_s\overrightarrow{M} \times \left(\vec{M} \times \vec{\sigma}\right)$ where M_s is the saturation magnetization, t is the thickness of the ferromagnetic cobalt layer, J_s the spin current, and $\vec{\sigma}$ the direction of spin polarization of the electrons at the platinum-cobalt interface. If an external magnetic field ($\vec{H}$) is

applied, the torque due to the magnetic field on the magnetization of the cobalt is given by $\overrightarrow{M} \times \left(\vec{M} \times \vec{H}\right)$. Overall, the magnetization dynamics under the influence of an external magnetic field and the spin torque is given by a modified Landau Lifschitz Gilbert equation[16]:

$$(1+\alpha^2)\frac{d\vec{M}}{dt} = -\gamma\left(\vec{M}\times\vec{H}\right) - \frac{\alpha\gamma}{M_s}\left(\vec{M}\times\vec{M}\times\vec{H}\right) - \frac{\gamma\hbar}{2eM_s t}\left(\vec{M}\times\vec{M}\times\vec{\sigma}\right)$$

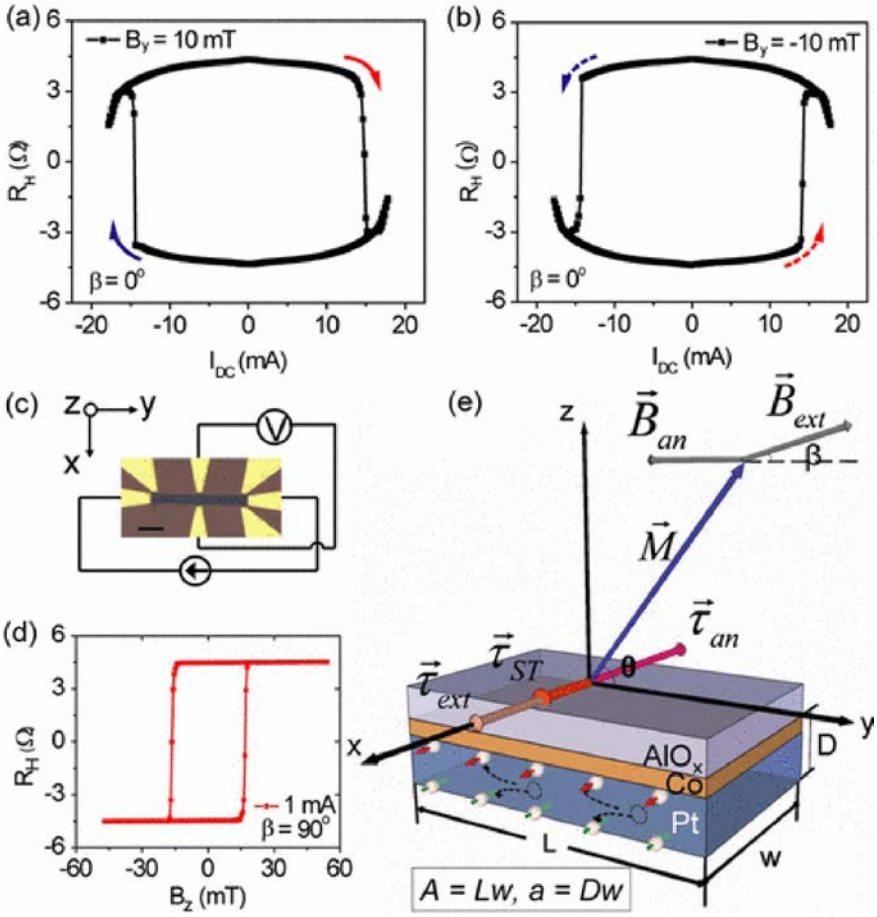

Figure 7: (a), (b) Current-induced switching in a Pt=Co=AlOx sample at room temperature in the presence of a small, fixed in-plane magnetic field B_y with (a) B_y = 10 mT and (b) B_y = 10 mT. (c) Top view of the sample (50 μm scale bar). (d) R_H as a function of B_{ext} perpendicular to the sample plane. (e) Illustration of the torques exerted by the external field B_{ext}, the anisotropy field B_{an}, and the SHE torque τ_{ST} for positive current, when B_{ext} and M are in the yz plane. The dashed arrows show the direction of electron flow for positive current. Reproduced from Liu et al in [15].

The work in [6] further explored perpendicular anisotropy magnet switching. The devices were again Hall bars, with the details and stack already given earlier in this report. Their work found that tantalum had a giant spin Hall Effect which could be effectively used to switch a magnet. A few other discoveries were made that are significant to this section and to this report in general. The current density in tantalum required to switch the magnet was less than their work on using the spin Hall Effect of platinum, leading to the conclusion that the spin hall angle of tantalum is

higher than that of platinum. That is to say, for a given current density, the magnitude of the spin current in the tantalum is larger than that in the platinum. Additionally it was noted that the sign of the switching was different. For a given field and current polarity, tantalum switches in the opposite direction of platinum. This led to the opposite sign of the spin Hall angle for tantalum and platinum.

In this section, a brief overview of the basics needed to understand the results listed later in this report was given. Understanding these basics will give the reader some idea of how the basic physics of the mechanism here function and how the reader might be able to implement these experiments. Furthermore, some discussion is given to differentiate between different switching mechanisms and different materials. Following this section, this report covers experiments based on the giant spin Hall Effect switching of tantalum and thus, this is the most important piece of information for understanding this report. Armed with the information of these previous sections, the reader can understand the observations, data, and experiments that follows and perhaps form hypotheses of his/her own.

3
Process Flow

This section will provide the overview for the process flow utilized in this project. Furthermore, a quick list of the measurements used will also be provided. The fabrication process utilized here required the use of the UC-Berkeley Nanolab fabrication facility for photolithography, photoresist spinning, sample cleaning, and development. Other work was done in other labs that were not a cleanroom environment. Finally, the devices were placed onto a chip carrier and wire bonded in order to provide proper electrical contacts.

3.1 Fabrication Process Flow

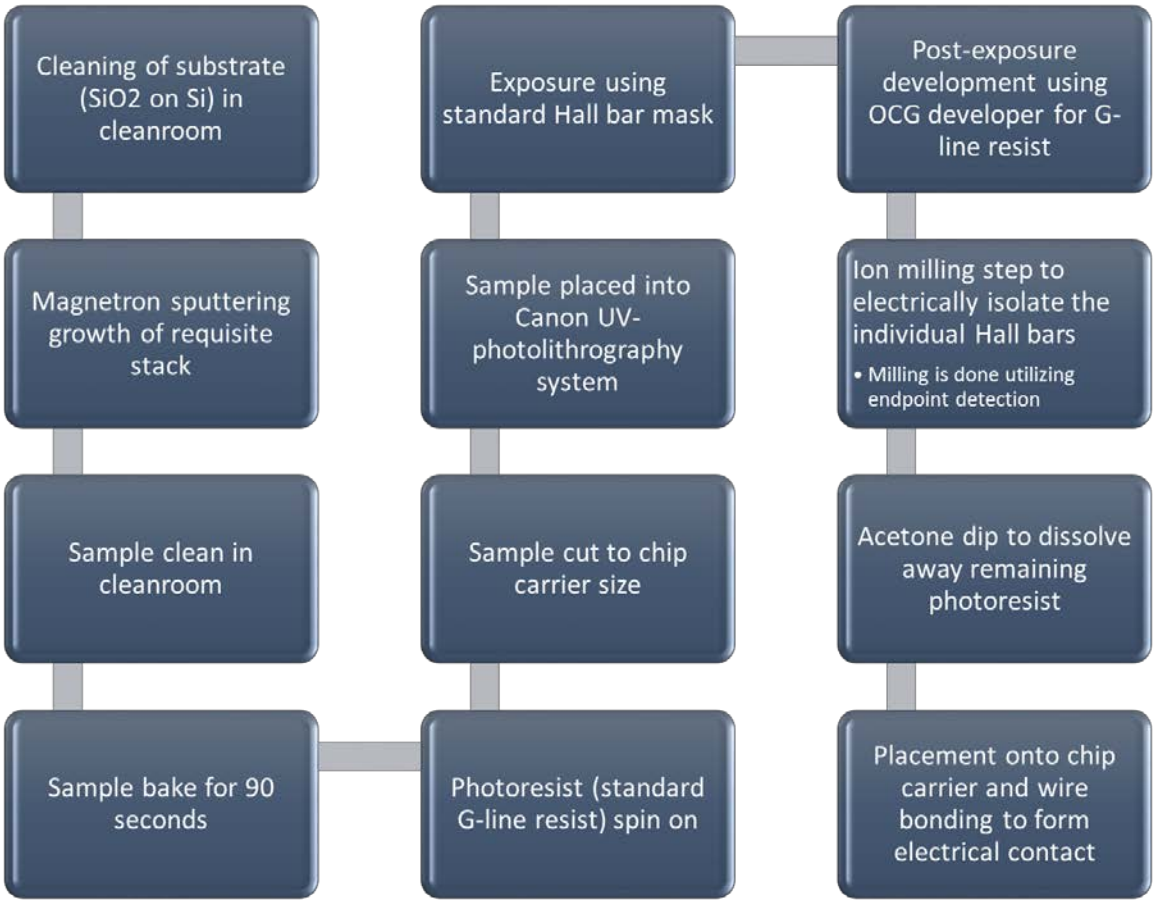

Figure 8: Process flow for the fabrication of Hall bars

Many of the steps here required careful calibration, testing, and adjustment for proper implementation. The reader should keep in mind that device fabrication often takes many steps and many tries. In particular here, the magnetron sputtering process required careful testing and adjustment. Proper sputtering of MgO requires sufficient target cleaning and was even found to have a certain “warm up” time after which the materials sputtering usually did not yield the

desired characteristics. Another interesting observation was the impact of rotation speed on the material quality. Specifically, in this project, out of plane anisotropy materials were desired. However, when the rotation speed was too slow, the materials featured a partial switch in magnetization at low fields and then required larger fields to complete saturate. This was attribute to multiple magnetic domains resulting from the slow rotation speed. The ion milling step was performed in order to electrically isolate the different Hall bars from each other by removing all the stack material in between. This was achieved by using a Hall bar mask and then ion milling until silicon was reached. The particular ion milling system used here had a secondary ion mass spectrometry endpoint detection system which aided this step as it could detect when the milling of silicon began. After careful fabrication, useful devices were made using the general process flow given here.

3.2 Measurements

Measurements are integrated throughout the process whether they are quick measurements to verify a fabrication step or a detailed measurement to characterize the fabricated devices. In this section, an overview of the measurements and the step at which they occur will be covered.

The first measurement step took place after the sputtering of the material in order to verify the magnetization type of the sample. That is to say, vibrating sample magnetometry was done to verify whether the samples indeed had the desired out of plane anisotropy. Sample curves for the films grown in this project are featured in figure 9.

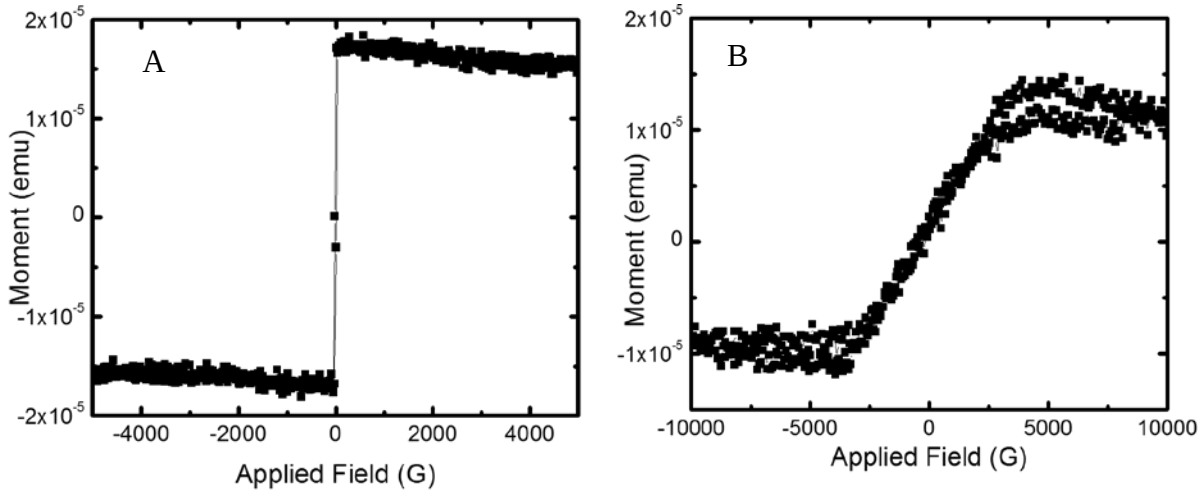

Figure 9: Hysteresis loops for a perpendicularly polarized film using VSM. A) Out of plane hysteresis loop. B) In-plane hysteresis loop

After characterization of the magnet anisotropy and verification that it is indeed out-of-plane, the sample is viable for fabrication. Following the process detailed in this report, the samples are then cleaned and cut in preparation for fabrication. After reaching the point of ion milling, the sample can be checked for proper isolation using a quick multimeter measurement. Then, the rest of the process can be completed. The final device is similar to the figure on the following page, except that in the devices used in this project, gold pads are not included. The sample featured in figure 10 is an earlier device, thus featuring the gold pads that were later done away with.

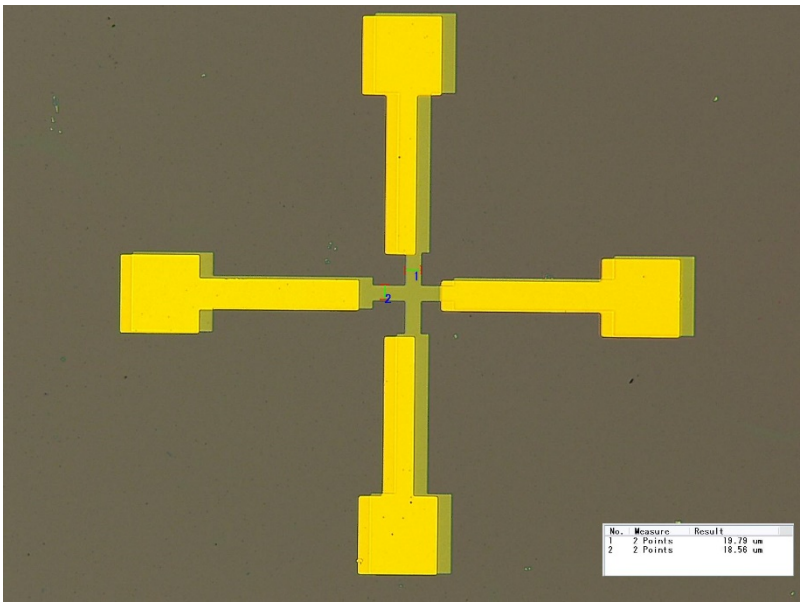

Figure 10: Microscope image of the Hall bars fabricated in this project. The average Hall bar width was 20 μm

Once fabrication is completed the final measurements are all done using a typical anomalous Hall Effect measurement system. First, a simple anomalous Hall Effect curve is swept out (see figure 11) and then the current switching measurements vital to this report are performed. A current is applied between 2 of the contacts and a voltage is measured between the other two contacts with a field applied out of the plane (for the anomalous Hall Effect) and in plane (for the switching measurements). For the switching measurements a small field is applied in plane and the current is applied along the field direction, with the voltage measured perpendicular to the current. The magnet was always reset into the "up" position before a current pulse was applied to switch. The measurements were performed to a certain degree of robustness with fifteen measurements done per sample. Figure 11 part b shows these switching measurements. The fifteen switching measurements were used to identify the current it took to reliably switch the samples. Later on, other measurements were performed for reliability analysis and heating, those will be discussed in a later section.

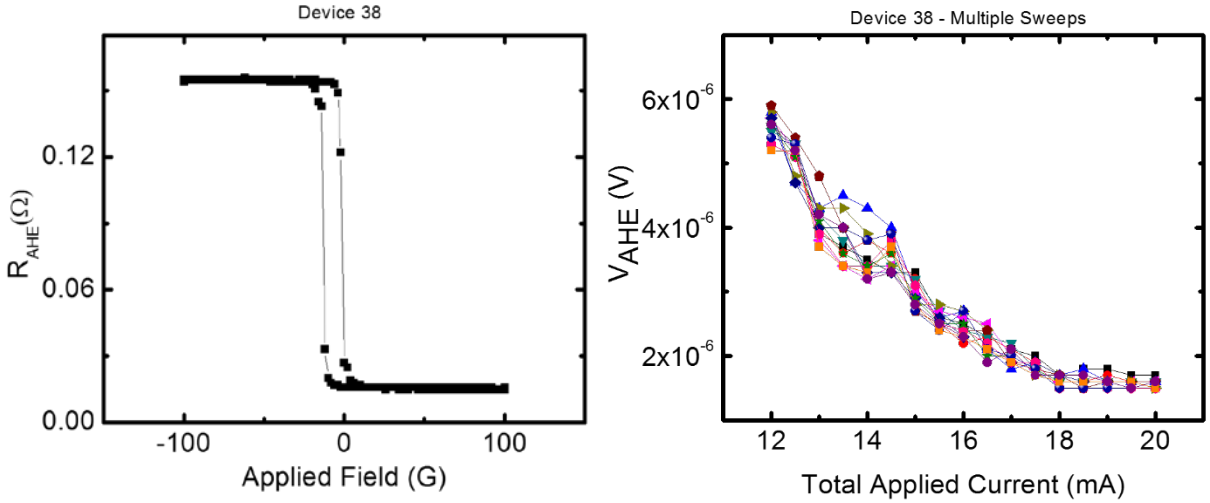

Figure 11: A) Anomalous Hall Effect curve for a sample and B) switching curve showing a reliable switching current of 18mA

4
Experiments & Results

4.1 Main Experiments and Results

In search for more efficient and effective ways of utilizing the spin Hall Effect spin torque of tantalum (or platinum), we explored the placement of these metals adjacent to each other in the stack. Specifically, thin film stacks of Ta(2)/Pt(x)/Ta(10-x)/CoFeB(1)/MgO(2)/Ta(2) were grown on Si/SiO_2 substrates with thicknesses in nanometers. A schematic of the stack structure is given in figure 12.

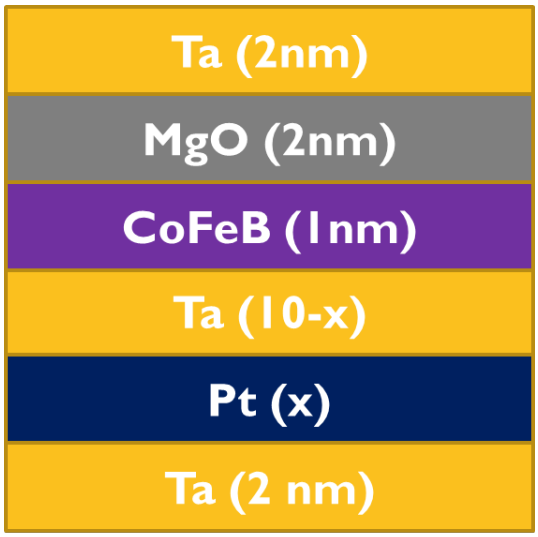

Figure 12: Thin film stack structure to utilize the spin Hall Effects of two metals with a perpendicular anisotropy magnet

The reasoning behind using this configuration was to create a non-equilibrium situation at the interface of platinum and tantalum to force new spin dynamics in the structure. The enhancement seen in the data is still anomalous however, since no theoretical results have been developed that explain the enhancement. The following stack structures were grown in order to explore the effects of having different thicknesses of platinum underlayer, all thicknesses in nanometers:

- Stack 37: Ta(2)/Pt(5)/Ta(5)/CoFeB(1)/MgO(2)/Ta(2)
- Stack 38: Ta(2)/Pt(3)/Ta(7)/CoFeB(1)/MgO(2)/Ta(2)
- Stack 40: Ta(10)/CoFeB(1)/CoFeB(1)/MgO(2)/Ta(2)
- Stack 59: Ta(2)/Pt(2)/Ta(8)/CoFeB(1)/MgO(2)/Ta(2)

Once the samples were grown by sputtering, VSM hysteresis loops were acquired for all the samples to verify their perpendicular anisotropy prior to fabrication. All samples were then fabricating using the process discussed in this report. Once wire bonding was completed, anomalous Hall Effect (AHE) measurements were performed on all the devices to make sure the anisotropy remained after fabrication. The curves for all these devices are included in figure 13.

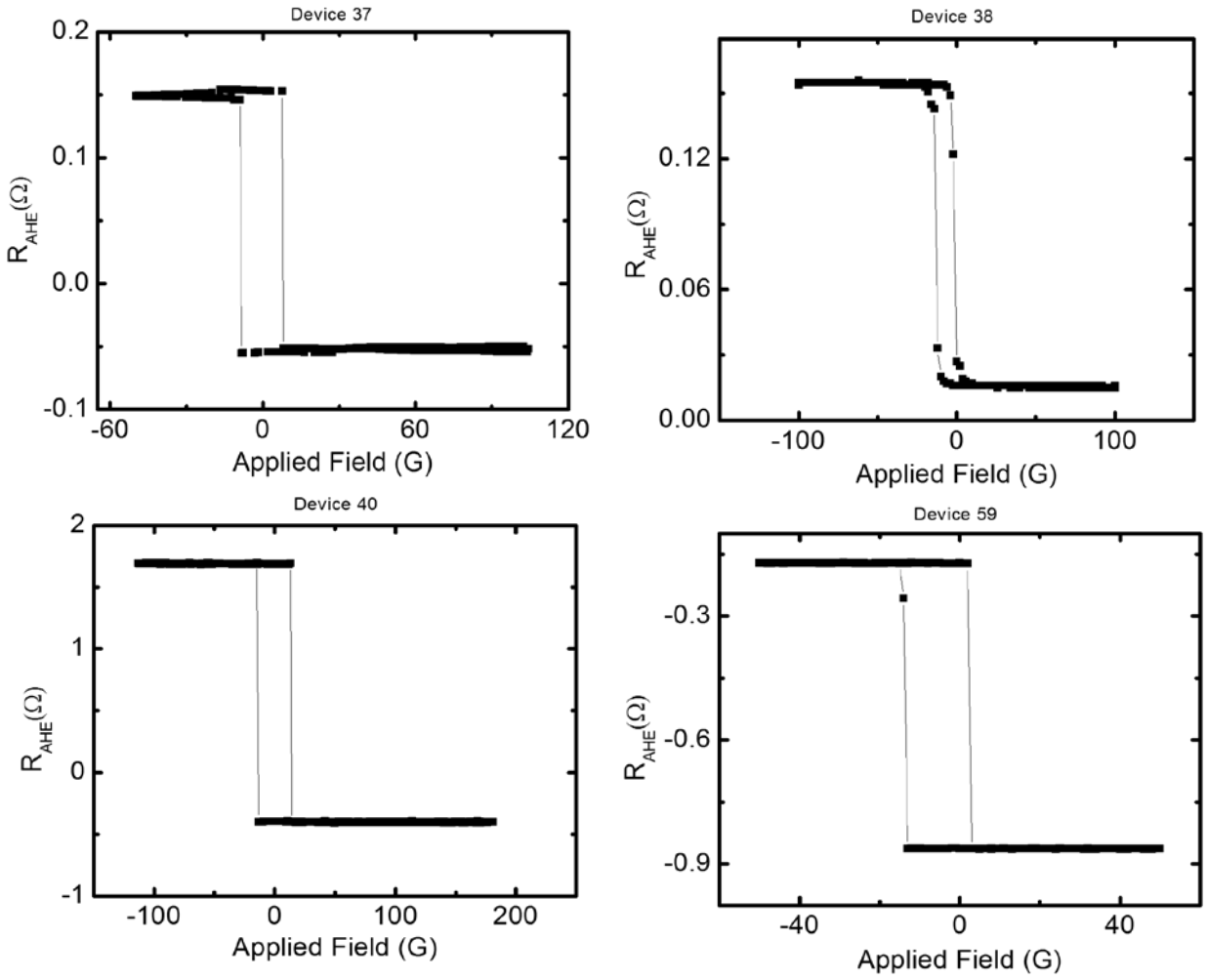

Figure 13: Anomalous Hall Effect curves for all four sample structures as listed. The curves show that all the samples have good out of plane anisotropy and thus all good samples for the experiment

After verifying the perpendicular anisotropy, the devices are ready to be tested utilizing the measurement previously mentioned. The measurements were repeated fifteen times to verify the switching currents and a typical plot looks like that in figure 11 b. The graph in figure 14 shows the initial results. At first glance, the results seem to indicate the exact opposite of what was desired. Rather than discovering a reduction of current with increasing platinum, a marked increase of switching current is observed. Initially disappointing, the realization was made that the absolute current increase was indeed due to the platinum layer. However, since the platinum resistivity is an order of magnitude lower than that of tantalum, the platinum shunts a great deal more of current than the tantalum layer, the layer which we are using to switch the adjacent magnet. Thus, an analysis was developed to calculate the current densities in each of the layers.

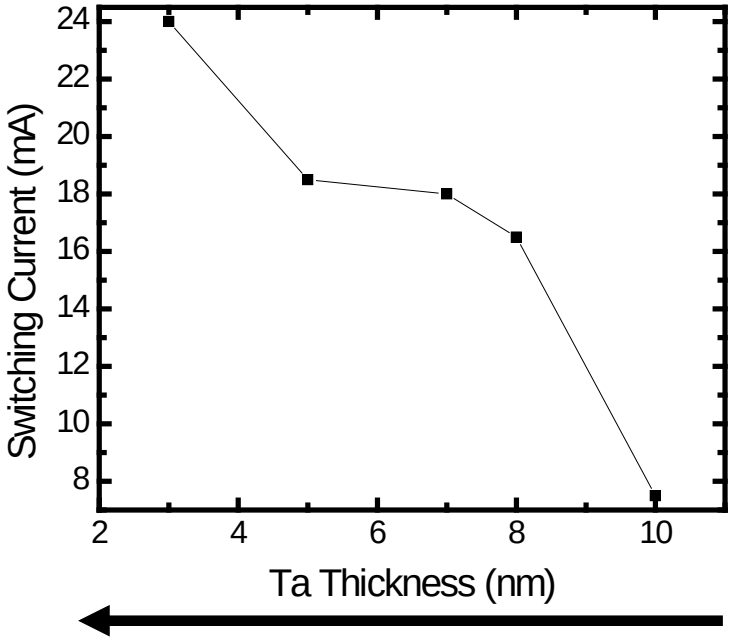

Figure 14: Plot of switching current vs. Ta Thickness

The analysis was performed by considering a parallel network of resistors for each of the metallic layers in the stack (all layers except for the MgO). Each metallic layer shunts a certain amount of current according to its resistivity and thickness. Using the resistivities of each layer and simple current divider calculation, the percentage of current passed through the tantalum and that shunted by platinum was calculated and this are included in figures 15 and 16.

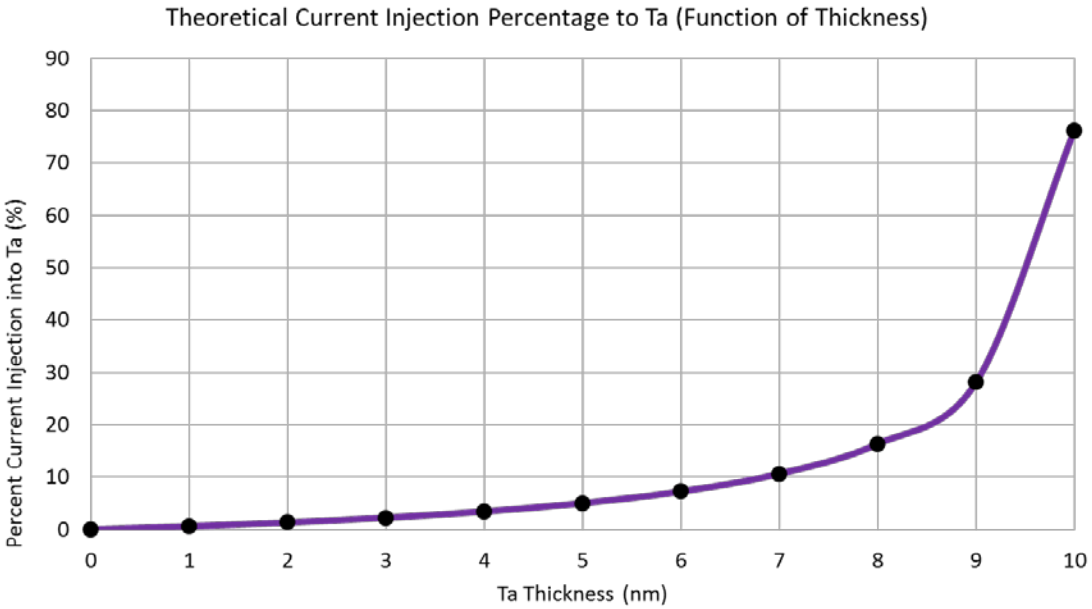

Figure 15: Plot of Percent Current Injected into Ta vs. Ta Thickness

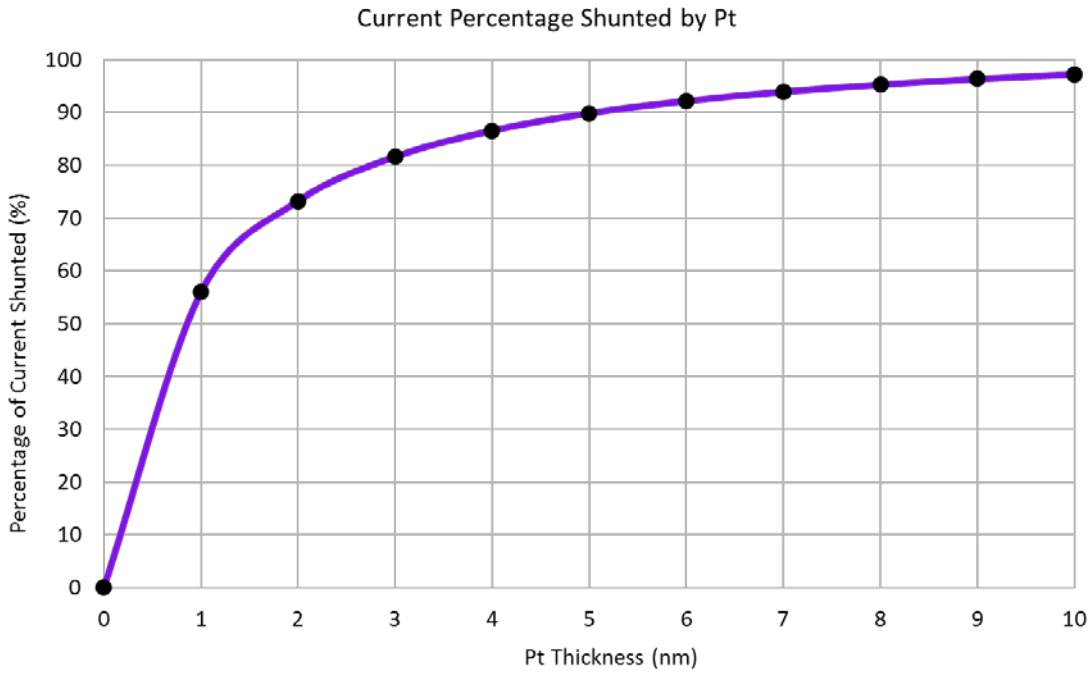

Figure 16: Plot of Percent Current Shunted By Platinum

These figures show that even for thin platinum thicknesses, the platinum shunts more current than is passed through the tantalum layer. This readily explains why it took more current to switch the samples with thicker platinum underlayer. Using the computed current percentages and normalizing with thickness and hall bar width, a current density through tantalum is computed. The figure on the following page (Figure 18) shows the switching results for each sample in terms of the tantalum current density. The results after the current density is computed are much more encouraging and yield useful results. Taking into account current shunting through the other layers, the current density required to switch is actually reduced with increasing platinum thickness. This is clear once the current density to switch is plotted against the tantalum thickness (figure 17).

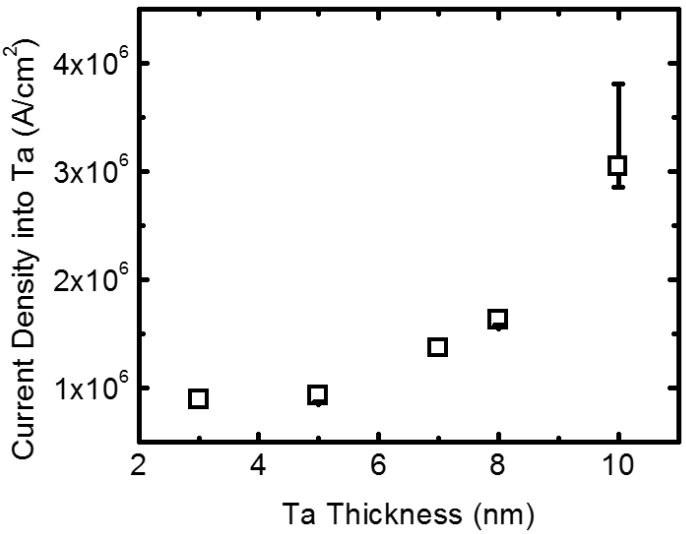

Figure 17: Plot of current density into Ta required to switch vs. Ta thickness. The trend shows that with decreasing tantalum thickness (increased platinum thickness) the current density into tantalum required to switch is decreased.

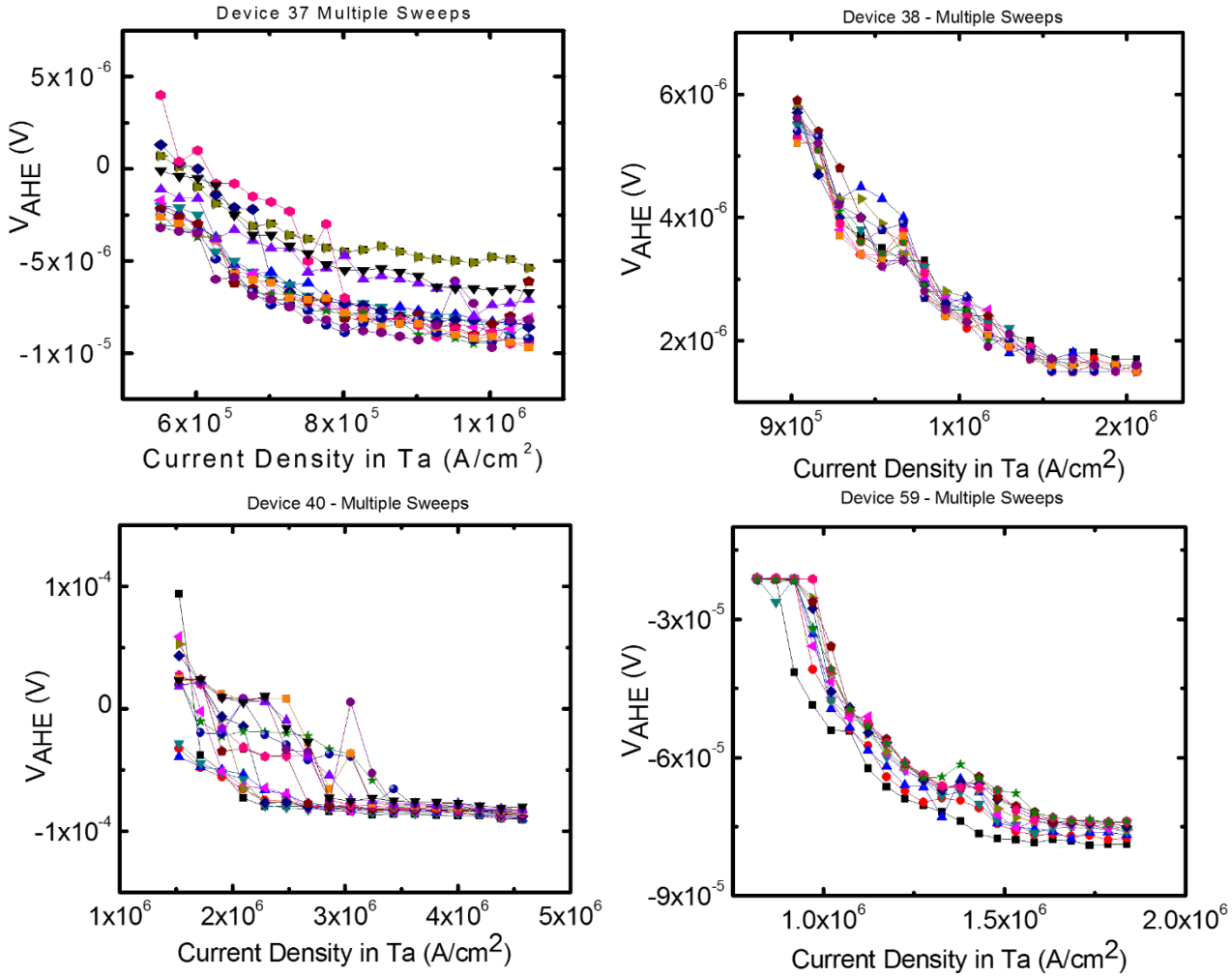

Figure 18: Switching curves for the four different samples listed.

Although the usefulness of the results does not immediately present itself, clear evidence has been shown that decreasing the tantalum thickness while placing a thicker platinum layer underneath decreases the required current density to switch the magnet. One point should be clarified that this is not the spin Hall Effect of platinum overcoming that of the tantalum. This can be observed the following two ways: the spin Hall angle of platinum is commonly given to be less than that of tantalum and secondly, the direction of switching would have reversed if the switching was occurring due to the platinum layer.

That being said, this effect can be immediately useful with other spin Hall Effect metals that have opposite signs. The effect discovered here would be better implemented if the two metals have similar resistivities. This can be done with tungsten which has been found to have the same spin Hall Effect sign as tantalum and tunable resistivity depending on its thickness[16]. Utilizing a material such as tungsten with another metal (such as platinum) could yield lower switching currents. This is a very viable direction for future research.

4.2 Examination of Potential Problems

Several issues can present themselves throughout the measurement process presented in this report. Measurements have been made in an attempt to address some of these problems and will be presented here in this section.

One of the first problems appearing during the testing of these spin Hall Effect devices was the changing in plane saturation field. Initially, it was not apparent whether this was a regular random fluctuation or a result of the different platinum underlayer thicknesses. Consequently, VSM measurements were completed on all the films to check the in plane saturation field. These measurements yielded the data in figure 19. Observing figure 19, one notices there is no trend between the current density required to switch and the in plane saturation field. Thus, it can be assumed that these are random fluctuations due to different growth conditions.

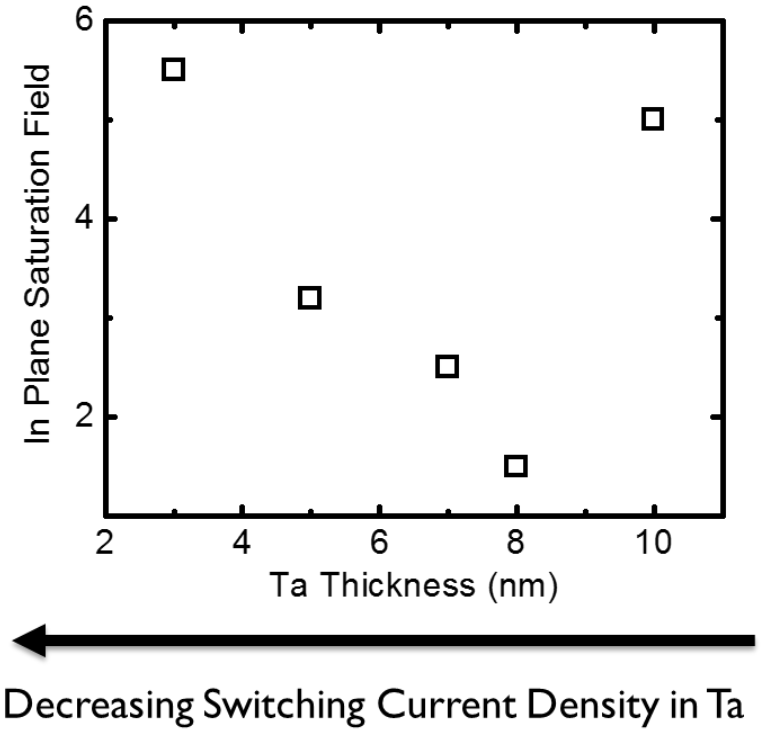

Figure 19: In Plane Saturation vs. Ta Thickness

Another measurement was made to measure the spin Hall angle according to the method used in [17]. This involves finding the change of the measured coercivity with different test current pulse magnitudes. The measured curves are seen in figure 20 and from the plot, the slope seems to be steeper than that in the reference but no calculation was made here since these measurements were not made on all devices. One immediate issue presenting itself in this measurement is heating of the device, causing a change in the measured anomalous Hall resistance.

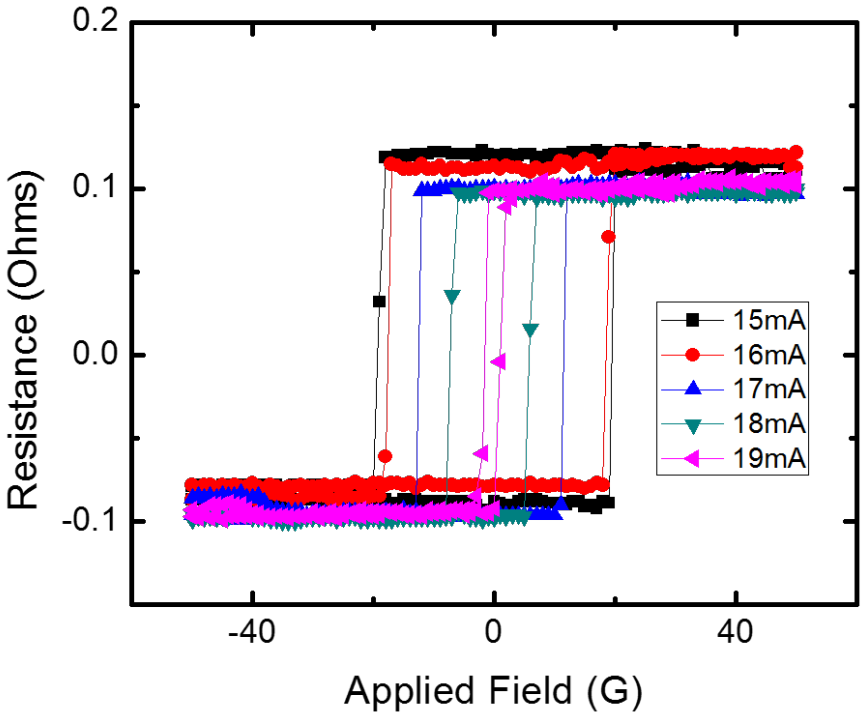

Figure 20: Anomalous Hall Effect hysteresis loops with different applied currents showing coercivity reduction with increased current

Since the stacks analyzed in this project involve increasing thicknesses of platinum underlayer (and thus decreased resistance) which would shunt more current, it is desirable to show that the switching happening in the devices is not due to heating. A marker of heating effects would be to see that as the platinum thickness increases, heating (based on I^2R) goes up. After performing resistance computations (taking into account the specific shape of the Hall bars used) and using the experimental switching current, the heating was actually found to slightly decrease with increasing platinum thickness (seen in figure 21). Thus heating is not a key issue causing the switching and it is likely that the switching is occurring due to the spin current. The current resistances used in the computations were purely based on theoretical values. A more accurate measurement for the heating effects would be to get the actual device resistances and use that to compute the I^2R based heating.

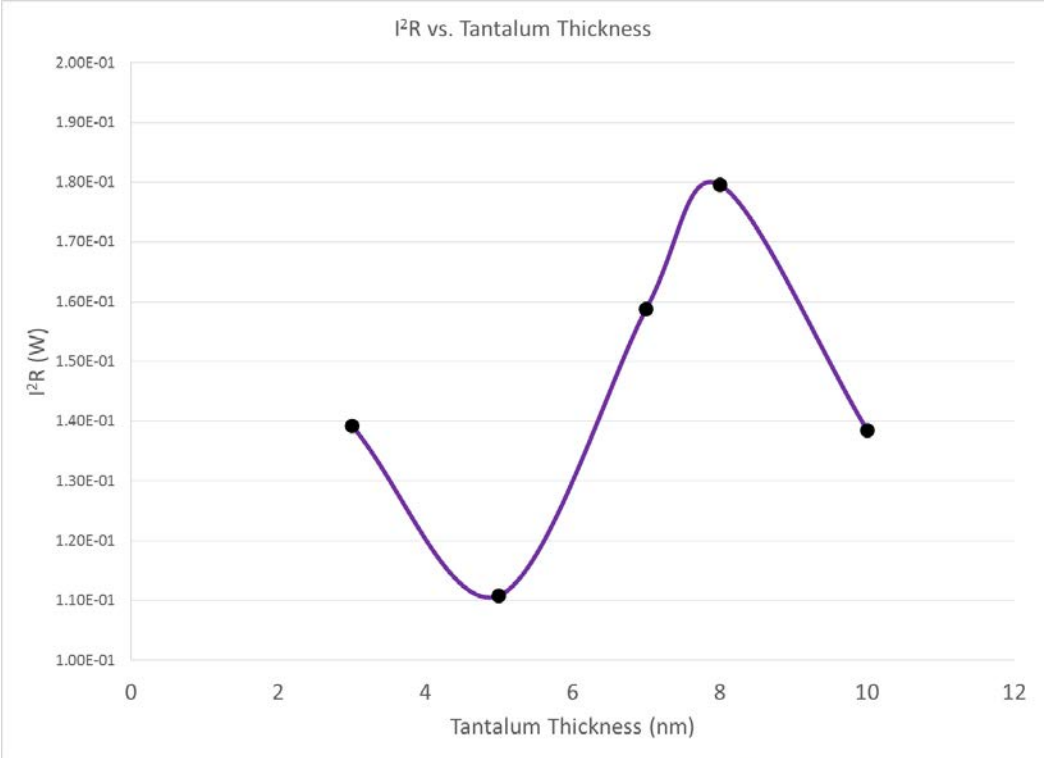

Figure 21: I^2R vs Tantalum Thickness plot to observe heating effects

Increasing Platinum layer thickness

The heating effects noted from figure 21 show that for increasing platinum layer thicknesses, the dissipation decreases until the lower tantalum layer thicknesses are reached. This is because as the tantalum layer thickness decreases, the effects of the tantalum seed layer and the tantalum capping layer begin to appear shunting more current. Overall the results in this section serve to support the notion that the placement of platinum is indeed resulting in anomalous enhancement of the spin Hall Effect and that no auxiliary effect is the source of the enhancement.

5
Conclusion

In conclusion, placing another metal with opposite sign of the spin Hall Effect under another spin Hall Effect metal can yield an improvement of the spin current. In the stacks tested here, Ta(2)/Pt(x)/Ta(10-x)/CoFeB(1)/MgO(2)/Ta(2), the current at first glance increases. However, analyzing the current density through the individual layers yields a decreased current density required for switching. Future work can improve upon this discovery by searching for materials where the resistivities of the two metals are similar, such that significant shunting does not occur by one of the metals. That would, theoretically, result in an enhancement of the actual applied current (decreasing it) and the spin current (increasing it). Although several other effects can potentially take place, systematic tests were performed to check for differences in the devices that could have resulted in the results found here. However, of all the tests, no significant evidence was found that the spin current was not in fact enhanced by the placement of another metal. However, there is still more testing to be done especially in terms of the device heating. Measuring the actual device resistances as well as actual temperature change could yield information useful for completing the analysis on whether or not heating effects are prevailing in these devices. Once all the information is compiled, these types of stacks could indeed be used to reduce switching current and thus, reduce the power consumption in future memory and other magnetic based technology.

References

[1] S. Ikeda, K. Miura, h. Yamamoto, K. Mizunuma, H.D. Gan, M. Endo, S. Kanai, J. Hayakawa, F. Matsukura, and H. Ohno. “A perpendicular-anisotropy CoFeB-MgO magnetic tunnel junction.” Nature Materials **9**, 721-724 (2010).

[2] S. Ikeda, J. Hayakawa, Young Min lee, F. Matsukura, Y. Ohno, T. Hanyu, and H. Ohno. “Magnetic Tunnel Junctions for Spintronic Memories and Beyond.” IEEE Transactions on Electron Devices **54**, 991-1002 (2007).

[3] P. P.J. Haazen, E. Mure, J.H. Franken, R. Lavrijsen, H.J. M. Swagten, and B. Koopmans. “Domain wall depinning governed by the spin Hall effect.” Nature Materials **12**, 299-303 (2013).

[4] J. Kim, J. Sinha, M. Hayashi, M. Yamanouchi, S. Fukami, T. Suzuki, S. Mitani, and H. Ohno. “Layer thickness dependence of the current-induced effective field vector in Ta|CoFeB|MgO.” Nature Materials **12**, 240-245 (2013).

[5] A. Brataas, A. Kent, and H. Ohno. “Current-induced torques in magnetic materials.” Nature Materials **11**, 372-381 (2012).

[6] L. Liu, C.F. Pai, Y. Li, H.W. Tseng, D.C. Ralph, and R. A. Buhrman. “Spin-Torque Switching with the Giant Spin Hall Effect of Tantalum.” Science **336**, 555-558 (2012).

[7] S. Woo, M. Mann, A. J. Tan, L. Caretta, and G. S. D. Beach. “Enhanced spin-orbit torques in Pt/Co/Ta heterostructures.” Applied Physics Letters **105**, 212404 (2014).

[8] W. Callister and D. G. Rethwisch. “Materials Science and Engineering: An Introduction, 8th Edition.” Wiley Publishing, December (2009)

[9] D. Bhowmik, O.J. Lee, L. You, S. Salahuddin. “Magnetization switching and domain wall motion due to spin orbit torque.” Chapter in “Nanomagnetic and Spintronic Devices for Energy Efficient Memory and Computing.” Wiley and Sons Publishing (2015 to be published).

[10] M. Morota, Y. Niimi, K. Ohnishi, D. H. Wei, T. Tanaka, H. Kontani, T. Kimura, and Y. Otani. “Indication of intrinsic spin Hall effect in 4d and 5d transition metals.” Physical Review B **83**, 174405 (2011)

[11] S. Zhang, P.M. Levy, and A. Fert. “Mechanism of Spin-Polarized Current-Driven Magnetization Switching.” Physical Review Letters **88**, 236601 (2002)

[12] A. Manchon. “Spin Hall effect versus Rashba torque: a Diffusive Approach.” Arxiv (2012).

[13]I. M. Miron, G. Gaudin, S. Auffret, B. Rodmacq, A. Schuhl, S. Pizzini, J. Voge;, P. Gambardella. “Current-driven spin torque induced by the Rashba effect in a ferromagnetic metal layer.” Nature Materials **9**, 230-234 (2010).

[14] P. Gambardella, I. M. Miron. “Current-induced spin-orbit torques.” Philosophical Transactions A **369**, 3175-3197 (2011).

[15] L. Liu, O. J. Lee, T. J. Gudmundsen, D. C. Ralph, R. A. Buhrman. “Current-Induced Switching of Perpendicularly Magnetized Magnetic Layers Using Spin Torque from the Spin Hall Effect.” Physical Review Letters **109**, 096602 (2012).

[16] C. F. Pai, L. Liu, Y. Li, H.W. Tseng, D.C. Ralph, R. A. Buhrman. “Spin Transfer Torque Devices Utilizing the Giant Spin Hall Effect of Tungsten.” Applied Physics Letters **101**, 122404 (2012).

[17] D. Bhowmik, L. You, S. Salahuddin. “Possible route to low current, high speed, dynamic switching in a perpendicular anisotropy CoFeB-MgO junction using Spin Hall Effect of Ta.” Electron Devices Meeting (2012).